Article

Cell Reports

CD40 Stimulation Obviates Innate Sensors and Drives T Cell Immunity in Cancer

Graphical Abstract

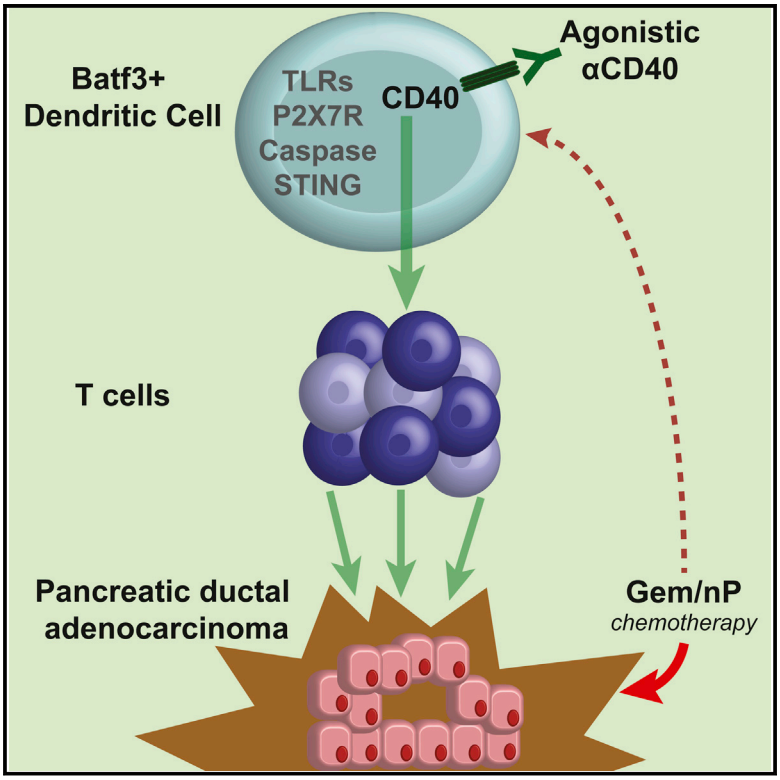

Authors

Katelyn T. Byrne, Robert H. Vonderheide

Correspondence

rhv@exchange.upenn.edu

In Brief

Immunologically "cold" tumors lack T cells and are hyporesponsive to immunotherapies. Byrne and Vonderheide show that CD40 stimulation, with chemotherapy, converts a "cold" tumor to a site of T cell infiltration and destruction with durable responses. Functional immune responses are independent of innate immune sensors important in other settings.

Highlights

- CD40 stimulation converts T-cell-deficient tumors to immunologically replete sites
- CD40 mediates clonal T cell expansion with decreased regulatory T cells
- Functional adaptive immune responses require both CD40 stimulation and chemotherapy
- Converted tumors undergo durable responses independently of innate immune sensors

Byrne & Vonderheide, 2016, Cell Reports *15*, 2719–2732
June 21, 2016
http://dx.doi.org/10.1016/j.celrep.2016.05.058

CellPress

Cell Reports
Article

CD40 Stimulation Obviates Innate Sensors and Drives T Cell Immunity in Cancer

Katelyn T. Byrne[1] and Robert H. Vonderheide[1,*]
[1]Abramson Cancer Center and Department of Medicine, University of Pennsylvania, Philadelphia, PA 19104, USA
*Correspondence: rhv@exchange.upenn.edu
http://dx.doi.org/10.1016/j.celrep.2016.05.058

SUMMARY

Cancer immunotherapies are more effective in tumors with robust T cell infiltrates, but mechanisms to convert T cell-devoid tumors with active immunosuppression to those capable of recruiting T cells remain incompletely understood. Here, using genetically engineered mouse models of pancreatic ductal adenocarcinoma (PDA), we demonstrate that a single dose of agonistic CD40 antibody with chemotherapy rendered PDA susceptible to T cell-dependent destruction and potentiated durable remissions. CD40 stimulation caused a clonal expansion of T cells in the tumor, but the addition of chemotherapy optimized myeloid activation and T cell function. Although recent data highlight the requirement for innate sensors in cancer immunity, these canonical pathways—including TLRs, inflammasome, and type I interferon/STING—played no role in mediating the efficacy of CD40 and chemotherapy. Thus, CD40 functions as a non-redundant mechanism to convert the tumor microenvironment immunologically. Our data provide a rationale for a newly initiated clinical trial of CD40 and chemotherapy in PDA.

INTRODUCTION

Innate immune cells utilize a number of receptors to detect danger signals liberated when large numbers of host cells die, such as after chemotherapy or radiotherapy in patients with cancer (Green et al., 2009). Dying tumor cells release intracellular components such as high-mobility-group box 1, ATP, and DNA, which are recognized, in turn, by receptors such as Toll-like receptor (TLR) 4 (Apetoh et al., 2007), P2X7 receptor (P2X7R) (Ghiringhelli et al., 2009), and stimulator of interferon genes (STING) (Deng et al., 2014) to regulate immune responses against tumors. Accordingly, a number of innate sensor agonists are being brought forward for investigation in cancer patients (Corrales and Gajewski, 2015; Kaczanowska et al., 2013; Rook et al., 2015).

It is well-known that some chemotherapies can enhance antitumor immunity, working most effectively in immunocompetent versus deficient hosts (Emens and Middleton, 2015; Zitvogel et al., 2008); however, some tumors, such as pancreatic ductal adenocarcinoma (PDA), are notoriously resistant to chemotherapy and despite aggressive treatment, the 5-year survival rate for patients with metastatic PDA is less than 5%. Immunologically, PDA is uncommonly infiltrated by effector T cells and expresses a relatively low burden of non-synonymous mutations that could serve as neo-epitopes (Alexandrov et al., 2013; Jones et al., 2008; Sausen et al., 2015), consistent with what has been termed an immunologically "cold" tumor (Sharma and Allison, 2015). Newer combinations of chemotherapy, such as gemcitabine (Gem) and nab-paclitaxel (nP), have shown clinical promise in metastatic PDA (garnering FDA approval in 2013), but objective tumor response rates remain low (23% of patients respond to Gem/nP, compared to 7% with Gem alone) (Von Hoff et al., 2013). Multiple hypotheses have been proposed to explain how nP improves responses against PDA, including SPARC-dependent (Alvarez et al., 2013; Von Hoff et al., 2011) or -independent (Neesse et al., 2014) mechanisms of stromal destruction, decreased levels of cytidine deaminase (Frese et al., 2012), and macropinocytosis by KRAS mutant tumor cells (Commisso et al., 2013). Although paclitaxel may activate macrophages as a lipopolysaccharide (LPS) mimetic that binds TLR4 (Ding et al., 1993)—which raises the hypothesis of an immune effect from adding nP—progression-free survival is extended by only 1.8 months with Gem/nP compared to Gem alone (Von Hoff et al., 2013) and without durable remissions in this disease.

To investigate immune mechanisms that could convert PDA tumors from T cell-devoid to T cell-replete—as a first step toward establishing immune sensitivity—we used the genetically engineered $Kras^{LSL\text{-}G12D/+}$;$Trp53^{LSL\text{-}R172H/+}$, Pdx1-Cre (KPC) mouse model of PDA, in which oncogenic $Kras^{G12D}$ and mutant $p53^{R172H}$ are under the control of Cre recombinase specifically expressed in the pancreas. KPC mice develop spontaneous PDA with 100% penetrance and faithful recapitulation of key features of human disease (Hingorani et al., 2005), including a dearth of non-synonymous mutations (similar to other KRAS-induced mouse models of cancer; Westcott et al., 2015) and minimal effector T cell infiltration (Clark et al., 2007). Although CD40 ligation enhances immune activation and maturation of antigen presenting cells (APCs) (Bennett et al., 1998; Ridge et al., 1998; Schoenberger et al., 1998), in tumor-bearing KPC mice, αCD40 alone achieves only transient tumor regressions on the basis of macrophage reeducation and not T cell immunity (Beatty et al., 2011). Because αCD40 combined with vaccines drives cytotoxic $CD8^+$ T cell responses in the context of cancer (Diehl et al., 1999; French et al., 1999; Sotomayor et al., 1999), we explored αCD40 combined with chemotherapy as an in vivo

vaccine (Nowak et al., 2003) against PDA. The inability of αCD40 (with or without Gem) to generate potent T cell mediated regressions of KPC tumors is mitigated upon the depletion of suppressive macrophage populations (Beatty et al., 2015). We hypothesized that adding nP to αCD40/Gem, taking advantage of potential immune stimulating effects of paclitaxel (Ding et al., 1993), might reeducate the suppressive macrophages and promote robust anti-tumor T cell immunity, bypassing the need for macrophage depletion in this system.

Here, we report that αCD40 and the combination of Gem/nP—but neither αCD40 nor chemotherapy alone—achieves T cell-dependent regression of established tumors in mice, an effect that requires IFN-γ and host CD40. Tumor regression was notably independent of multiple innate sensing pathways that have been classically described as mediating both spontaneous and therapy-induced cancer immunity. These preclinical data provide the mechanistic rationale for a newly initiated clinical trial of Gem/nP/CD40 therapy in patients with PDA (http://www.clinicaltrials.gov, #NCT02588443).

RESULTS

Chemotherapy Requires the Addition of αCD40 for Regression and Cure of Established PDA in a T Cell-Dependent Manner

We harvested a spontaneous PDA tumor from a C57BL/6 KPC mouse and generated a cell line (4662) with mutant KRAS and P53 that grew progressively upon subcutaneous implantation in wild-type syngeneic hosts with extensive desmoplastic stroma in the tumor microenvironment (TME) (Lo et al., 2015). Treatment of established 4662 tumors on day 12 with αCD40 and Gem/nP achieved significant regressions 12–14 days later (median regression rate across experiments, 59.7% ± 26.0%), whereas only rare regressions were observed in mice treated with Gem/nP or αCD40 alone (Figure 1A). Additionally, the overall tumor growth rate was significantly reduced in Gem/nP/αCD40 treated mice compared to mice treated with Gem/nP or αCD40 alone (Figure 1B). Similar results were found with a second desmoplastic PDA cell line (G43) also derived from a C57BL/6 KPC mouse (Figure S1). Gem/nP/αCD40 treated mice had significantly enhanced overall survival, with 14.7% (versus 0%) of mice being cured (Figure 1C). A second dose of Gem/nP 7 days later (day 19), to mimic the weekly dosing schedule in the clinic (Beatty et al., 2013; Von Hoff et al., 2013), neither enhanced nor hindered the rate of regression (Figure S2). Mice that were cured of the primary tumor with Gem/nP/αCD40 treatment rejected both 4662 and G43 tumor cells when injected 60 days or more later (Figure 1D and data not shown). This effect reflected T cell-mediated memory against PDA, as mice cured with Gem/nP/αCD40 and then depleted of $CD8^+$ T cells after 60 days quickly succumbed to tumor if rechallenged (Figure 1D). Depletion of either $CD4^+$ or $CD8^+$ T cells, or both, before initial treatment with Gem/nP/αCD40 also abrogated the response to therapy (Figure 1E). Thus, in contrast to the macrophage-dependent response generated with αCD40 monotherapy, the combination of both Gem/nP and αCD40, but neither alone, effectively mediated T cell-dependent regressions of PDA, reducing overall tumor growth and enabling long-term cures.

Gem/nP/αCD40 Therapy Skews the PDA Microenvironment in Favor of Effector T Cells

Given that T cells mediated tumor regressions prominently on day 23–25, we investigated $CD4^+$ and $CD8^+$ T cell subsets in the TME at this time point. The prevalence of effector T cells was similar or slightly increased with Gem/nP/αCD40 compared to Gem/nP or αCD40 alone (Figure 2A), but $FoxP3^+$ T regulatory cells (T_{Regs}), comprising nearly 20% of total $CD3^+$ T cells in vehicle or Gem/nP treated mice (data not shown), was significantly reduced after treatment with αCD40 and nearly completely eliminated with the addition of Gem, nP, or both (Figure 2B). As a result, the effector T cell:T_{Reg} ratios were significantly skewed in favor of both $CD4^+$ and $CD8^+$ effector T cells in the TME after αCD40 (Figure 2C), independently of the addition of Gem and/or nP. The significant reduction in T_{Regs} after αCD40 therapy was observed in both the proportions and in the absolute number of T cell subsets (Figure 2C and data not shown). $CD4^+$ T cell subsets in the TME were significantly altered as early as 5 days after αCD40, when the proportions of $FoxP3^+$ and $GATA3^+$ $CD4^+$ T cells were significantly reduced in Gem/nP/αCD40 treated mice, concurrent with an increase in $ROR\gamma t^+$ and $Tbet^+$ $CD4^+$ cells (Figure 2D).

αCD40 Therapy Increases the Clonal T Cell Response against PDA

To further investigate the effects of αCD40 on the T cell repertoire, we performed T cell receptor (TCR)-β chain CDR3 region deep sequencing to track unique T cell clones in tumors harvested from mice treated with Gem/nP/αCD40, αCD40 alone, Gem/nP alone, or vehicle control. To differentiate the effect of each therapy on the TCR repertoire, mice were grouped by αCD40 treatment (Figures 2E and 2F, top) or Gem/nP treatment (bottom) and analyzed by machine learning using random forest classification (RFC), as we have previously reported (Twyman-Saint Victor et al., 2015). This unbiased analysis approach successfully segregated mice based on αCD40 therapy, regardless of Gem/nP treatment, indicative of the impact of CD40 stimulation (but not chemotherapy) on clonal T cell responses in the TME. Among all mice that received αCD40, the cumulative proportions of rare and small clones (those found at a frequencies <0.01%) were significantly increased and hyperexpanded clones (highly represented clones in the TME) were moderately increased, compared to mice that did not receive αCD40 (Figure 2E, top). In comparison, the cumulative frequencies of rare to hyperexpanded clones remained constant when mice were segregated by chemotherapy treatment only, regardless of CD40 treatment (Figure 2E, bottom). The moderate increase of hyperexpanded clones in αCD40 treated mice significantly impacted the diversity of the most prevalent clones within the TME, such that the true diversity (measuring the effective number of clones) was increased for the top 10 and 20 clones within the TME, but not for the entire T cell population (Figure 2F, top). Thus the Gini coefficient (clonality) was significantly increased for the entire response after αCD40 therapy (Figure 2F, top), reflecting the expansion of the most frequent clones in the TME. Again, only exposure to αCD40 and not chemotherapy impacted these diversity and clonal metrics (Figure 2F, bottom). Furthermore, these changes were only observed in the TME itself; using the

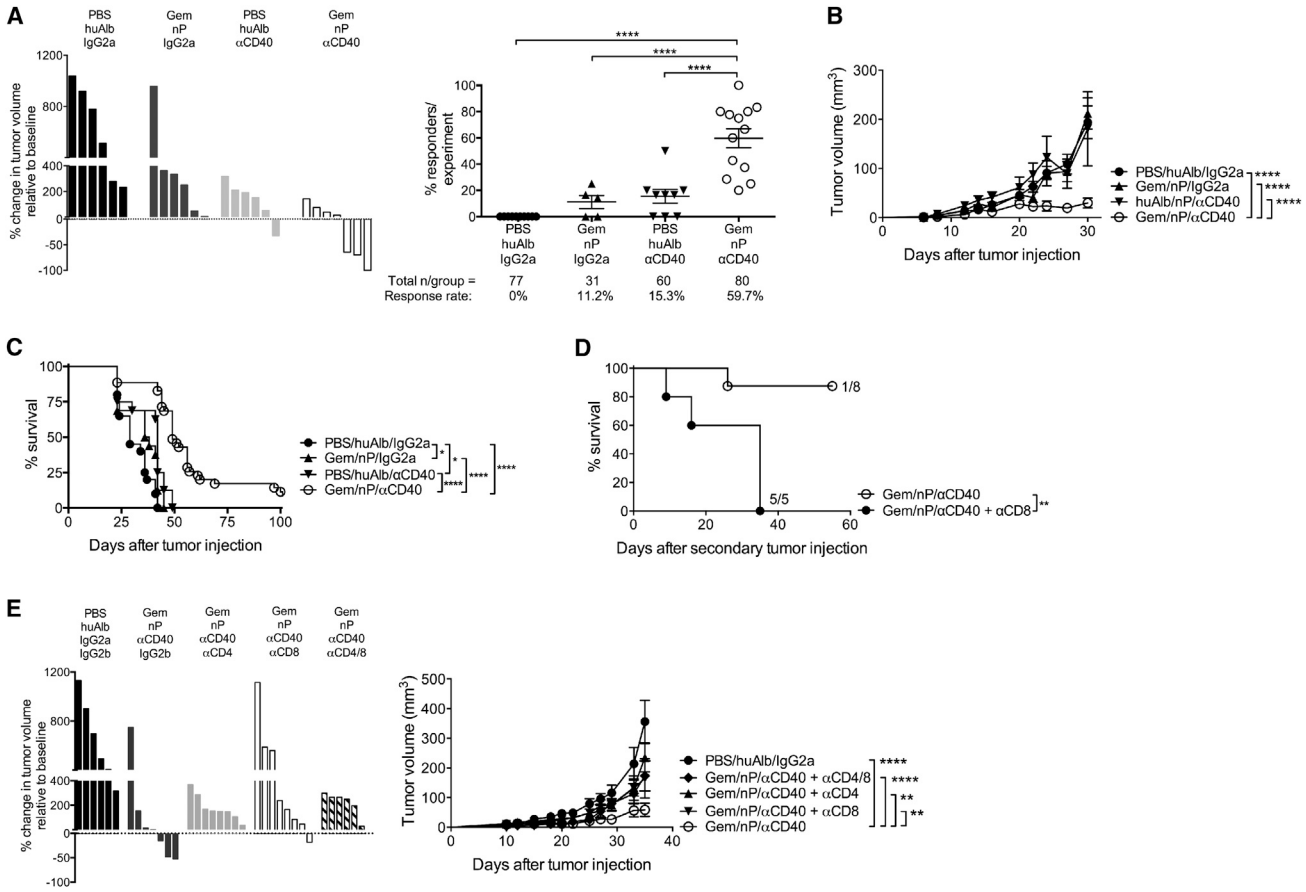

Figure 1. Gem/nP/αCD40 Drives T Cell-Dependent Regressions of PDA

Mice were injected with PDA 4662 cells subcutaneously and, after 12 days of growth, tumors were treated with Gem/nP followed by αCD40 2 days later.

(A) Left, change in tumor volume on day 24 compared to start of treatment (day 12), representative of seven independent experiments. Right, the total proportion of regressors/experiment, from 13 individual experiments, with the total number of mice/group shown below.

(B) Tumor growth kinetics for mice from (A).

(C) Survival curve for mice treated as described in (A), from two combined experiments.

(D) Survival after second tumor injection >60 days after primary tumor injection. Some mice received αCD8, representative of two independent experiments.

(E) Mice were treated as described in (A), and with αCD4 and/or αCD8. On the left, the change in tumor growth compared to baseline is shown, and, on the right, tumor growth kinetics are shown. The data are representative of three independent experiments.

Each experiment had 4–10 mice/group, each bar represents a single mouse, and each symbol represents a group, the horizontal line and error bars indicate mean ± SEM. The statistical analyses by one-way ANOVA (A), two-way ANOVA with Tukey's HSD post test (B and E), or log-rank test (C and D) are shown. See also Figures S1 and S2.

same machine-learning analysis in the spleen revealed no changes in the clonality or diversity of the T cell repertoire with either Gem/nP or αCD40 (data not shown). Therefore, αCD40 was independently associated with two significant changes in the TCR repertoire specifically within the TME: expansion of certain T cell clones and recruitment of new populations of rare and small clones to the TME.

Functional Effector T Cells Require Both Gem/nP and αCD40 Treatment

Although αCD40 independently mediated alterations in $CD4^+$ and $CD8^+$ T cell subsets, the addition of Gem/nP was required for increased functionality of the T cell compartment and control of tumor growth. $CD4^+$ T cell production of IFN-γ, TNF-α, and IL-2 was significantly increased in Gem/nP/αCD40 treated tumors compared to other groups (Figure 2G, left). Moreover, a higher proportion of $CD8^+$ T cells produced TNF-α or IFN-γ, or both cytokines, from tumors of mice treated with Gem/nP/αCD40 compared to Gem/nP or αCD40 alone (Figure 2G, right). Thus, αCD40 significantly reduced the T_{Reg} population and enhanced Th1 and Th17 subsets of $CD4^+$ T cells, but the development of functional effector $CD4^+$ and $CD8^+$ T cells was dependent on the addition of Gem/nP to αCD40.

IFN-γ Is Required for Gem/nP/αCD40 Efficacy

Given the increase in IFN-γ production by both $CD4^+$ and $CD8^+$ T cells, we investigated the role of IFN-γ in mediating Gem/nP/αCD40-treatment induced immune responses to PDA. In IFN-γ knockout (KO) hosts bearing established tumors, response to Gem/nP/αCD40 therapy at 24 days was fully abrogated

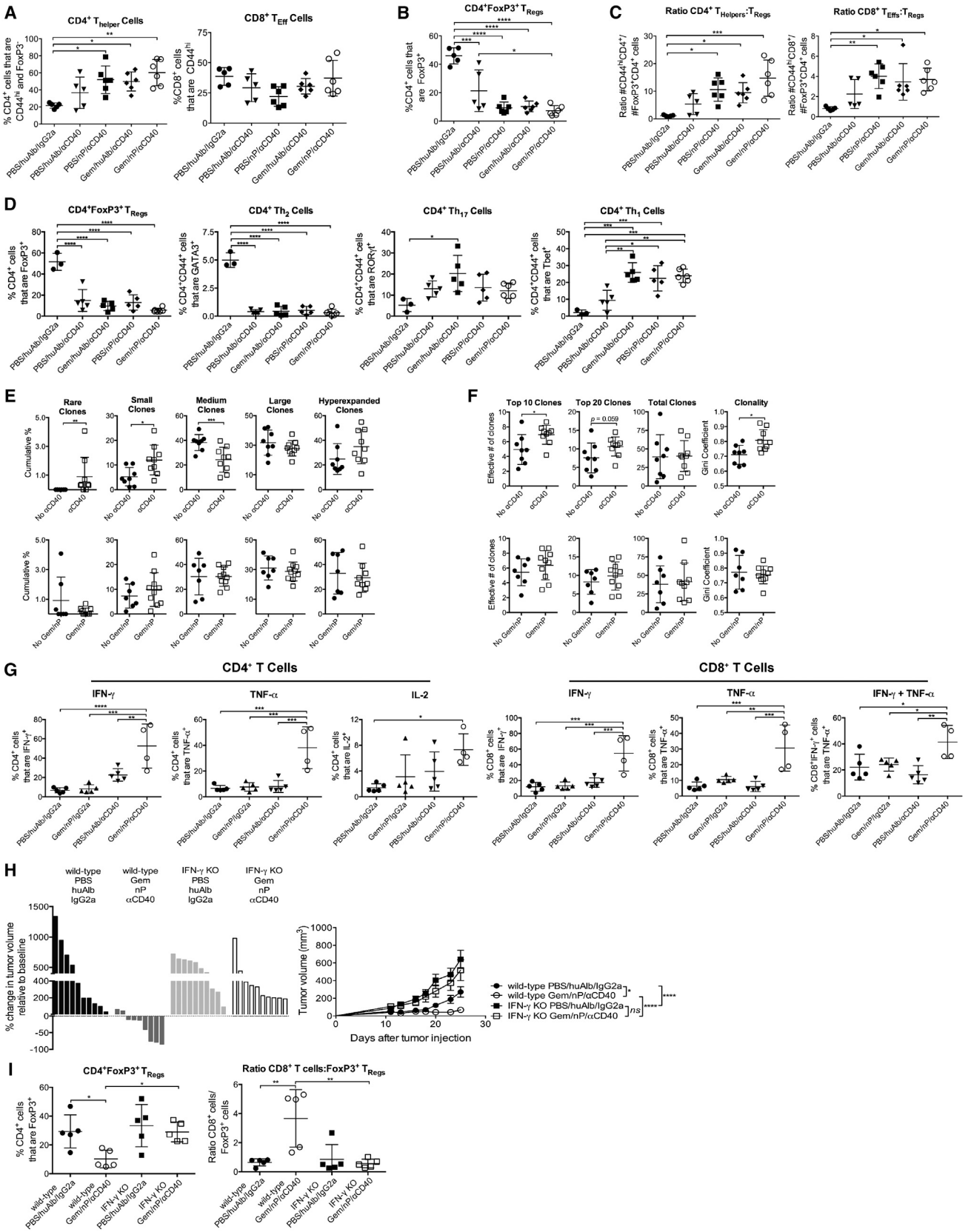

(legend on next page)

(Figure 2H, left). Although vehicle-treated tumors grew somewhat faster in IFN-γ KO mice versus wild-type mice, there was no reduction in tumor growth rate when IFN-γ KO mice were treated with Gem/nP/αCD40 (Figure 2H, right). IFN-γ is unlikely to be derived from the natural killer cell compartment because depletion with αNK1.1 did not alter tumor responses or growth rates in Gem/nP/αCD40 treated mice (Figure S3). Additionally, the intratumoral T_{Reg} compartment in IFN-γ KO mice was not significantly reduced after treatment with Gem/nP/αCD40 as it is in wild-type mice, and consequently the $CD8^+$ T cell:T_{Reg} ratio was not skewed in favor of effector T cells (Figure 2I), indicating a failure to generate effector T cells. The potent immune response generated against PDA after Gem/nP/αCD40 was therefore dependent on IFN-γ for mediating tumor regressions and for skewing the TME in favor of effector T cells.

Host CD40 Requirement and Increased Activation of Antigen-Presenting Cells after Treatment with Gem/nP/αCD40

To test the mechanism by which CD40-induced immunity is potentiated by Gem/nP, we treated tumor-bearing CD40 KO mice with Gem/nP/αCD40 therapy and observed no tumor regressions or reduction in overall tumor growth rates (Figure 3A). T_{Reg} reduction and skewing toward effector CD8 T cells at day 24 was also lost in the absence of host CD40 (Figure 3B). Because CD40 KO hosts lack functional germinal center formation for the generation of thymus-dependent B cell responses, we evaluated whether the lack of Gem/nP/αCD40 efficacy in CD40 KO hosts was due to a defect in the B cell compartment. We measured tumor response rates and growth rates in μMT KO mice (which lack mature B cells), but found these were similar to those in wild-type mice (Figure 3C). Thus, host expression of CD40 is required for the efficacy of Gem/nP/αCD40 therapy.

Following treatment with Gem/nP, tumor cell death increased 6 hr later (Figure S4) (Frese et al., 2012), suggesting potential liberation of tumor antigens in vivo prior to αCD40. At 3 days after chemotherapy administration (24 hr after αCD40), the proportions of activated, $MHCII^+$ $CD86^+$ $CD11b^+$ myeloid cells in the TME were significantly increased in Gem/nP/αCD40 treated mice compared to other groups, including αCD40 alone (Figure 3D). This increase in activated populations was also observed in $CD11b^+$ $F4/80^+$ macrophages and $CD11b^-$ $CD11c^+$ dendritic cells (DCs) from Gem/nP/αCD40 treated mice compared to Gem/nP or αCD40 alone (Figure 3D), and was mostly lost by day 5 (72 hr after αCD40 administration) (data not shown). The proportion of DCs, myeloid cells, and macrophages producing IL-12 in Gem/nP/αCD40 treated mice were also increased compared to Gem/nP or αCD40 alone (Figure 3E). We observed a concomitant decrease in IL-10 production by $CD11b^+$ $F4/80^+$ TAMs, $CD11b^+$ $Ly6C^+$ $Ly6G^+$ myeloid derived suppressor cells, and $Ly6C^{hi}$ $CD11b^+$ inflammatory macrophages (Figure 3F). Thus, Gem/nP/αCD40 therapy uniquely and significantly enhanced the activation status and function of APCs and myeloid cells in the TME.

$Batf3^+$ DCs Mediate Gem/nP/αCD40 Efficacy

To ascertain the role of APC subsets in mediating Gem/nP/αCD40 tumor regression, we treated Batf3 KO mice (which lack cross-presenting $CD8\alpha^+$ DCs) with Gem/nP/αCD40 and observed no tumor regressions and a significant diminution in overall tumor growth control (Figure 3G). We also targeted the phagocytic and myeloid cell populations using seven independent depletion methods including clodronate-encapsulated liposomes (Table S1), and although we observed a 30%–50% reduction in the target cell populations in the TME, we were unable to detect any change in treatment efficacy (data not shown and Winograd et al., 2015). Therefore, the effect of Gem/nP/αCD40 therapy required cross-presentation of tumor antigens by DCs for optimal immune responses against PDA.

Gem/nP/αCD40 Therapy Drives $CD8^+$ T Cell-Mediated Regression of Spontaneous PDA

Although 4662 subcutaneous tumors grow with extensive desmoplastic stroma reminiscent of primary PDA (Lo et al., 2015), we also studied Gem/nP/αCD40 treatment against autochthonous tumors arising spontaneously in KPC mice. Mice were enrolled after the diagnosis of a tumor (median volume 103 mm^3, range 30–400 mm^3) and treated with Gem/nP on day 0 and day 7 and αCD40 on day 2. Tumor-bearing KPC mice treated with Gem/nP/αCD40 exhibited a 35.7% total response rate, with tumor regressions in 3/14 mice and stable disease in 2/14 (Figure 4A). In comparison, KPC mice treated with vehicle control, or with the combination of Gem/nP, had no regressions or stabilization of disease, and only 1/14 mice treated with

Figure 2. Gem/nP/αCD40 Therapy Alters T Cell Subsets, Repertoire, and Function in PDA Tumors in an IFN-γ-Dependent Manner

(A–D) Mice were treated as described in Figure 1A, and tumors were harvested 24 days (A–C) or 19 days (D) after tumor injection (12 and 7 days after initiation of treatment, respectively) and analyzed by flow cytometry with regard to the proportion (A, B, and D) of the indicated subsets or the ratios of the absolute number of cells/gram of tumor (C) among live, $CD45^+$ $CD3^+$ cells.

(E and F) Tumors were harvested on day 24 and analyzed by TCR deep sequencing. Mice are grouped based on receiving CD40 (top) or Gem/nP (bottom), and the cumulative frequencies of Rare (representing $<10^{-5}$ total clones), Small (10^{-5} to $<10^{-4}$), Medium (10^{-4} to $<10^{-3}$), Large (10^{-3} to $<10^{-2}$), or Hyperexpanded (10^{-2} to 1) clones within the total repertoire are indicated (E), or the repertoire diversity ("true diversity," indicating effective number of clones) for the top 10, top 20, or entire population (far left to middle right), or the Gini coefficient (0 indicating polyclonal and 1 indicating monoclonal) on far right (F).

(G) Tumors were harvested at day 24 and analyzed by flow cytometry with regard to the indicated parameters among $CD4^+$ (left) or $CD8^+$ (right) live, $CD45^+$ $CD3^+$ cells.

(H) IFN-γ KO mice were treated as described in Figure 1A. The change in tumor volume on day 24 (left) with growth kinetics (right) are shown.

(I) Tumors were analyzed on day 24 by flow cytometry with regard to the indicated subsets or ratios among live, $CD45^+$ $CD3^+$ cells.

Each symbol represents an individual mouse, the horizontal lines indicate mean ± SD (A–G and I) except for (H), where each bar represents a single mouse and each symbol represents a group with mean ± SEM. The data are representative of 3–5 independent experiments with 4–6 mice/group, except TCR deep sequencing data, which is one experiment with 8–9 mice/group. The statistical analysis was performed by one-way ANOVA (A–D, G, and I), Mann-Whitney t test (E and F), or two-way ANOVA (H) with Tukey's HSD post test. See also Figure S3.

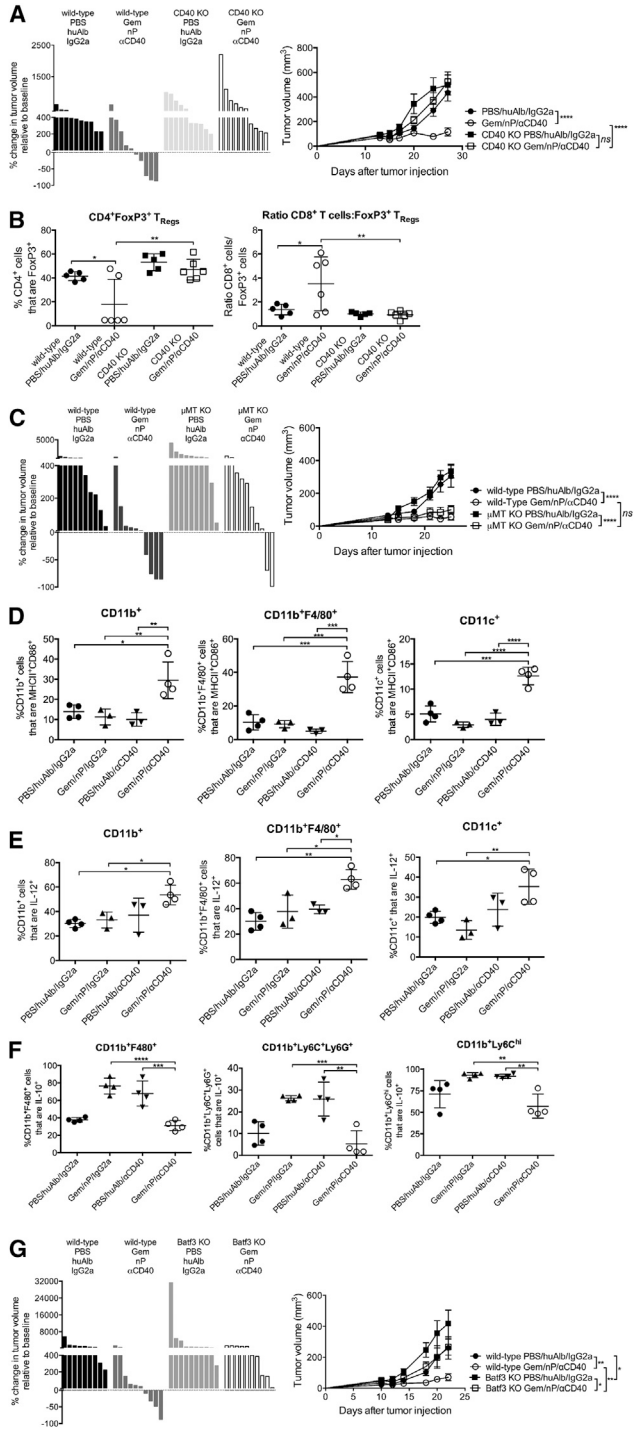

Figure 3. Gem/nP/αCD40 Therapy Requires Host CD40, Activates Antigen-Presenting Cells, and Requires Batf3⁺ Dendritic Cells for Efficacy

Mice were treated as described in Figure 1A.

(A and B) CD40 KO mice.

(A) Left, change in tumor volume on day 24 versus day 12 (start of therapy). The tumor growth kinetics are shown on the right.

(B) Tumors were analyzed on day 24 with regard to the proportions of indicated cells and ratios among live, CD45⁺ CD3⁺ cells.

αCD40 alone had stable disease at the 14-day time point after the start of therapy (Figures 4A and 4B). The previously reported 30% rate of regressions to αCD40 observed in tumor-bearing KPC mice (Beatty et al., 2011) was not observed here using KPC mice that are fully C57BL/6 backcrossed, although a recent report confirms the macrophage-dependency of αCD40 monotherapy in this strain of mice (Long et al., 2016). Moreover, in contrast to the previously reported macrophage-dependent (T cell-independent) regressions in KPC mice treated with CD40 alone (Beatty et al., 2011), here, the response rate was completely lost if mice treated with Gem/nP/αCD40 were first depleted of CD8⁺ T cells (Figures 4A and 4B), indicating a shift to a T cell-dependent immune response against spontaneous PDA when combining both Gem and nP with αCD40.

CD8⁺ T cell infiltration of the spontaneous PDA TME was significantly increased in KPC mice treated with Gem/nP/αCD40 in comparison to Gem/nP or αCD40 alone (Figure 4C, quantified on right). Additionally, the number of tertiary lymphoid structures (a biomarker of increasingly appreciated immunological importance, Dieu-Nosjean et al., 2014; Lutz et al., 2014) was significantly increased in spontaneous PDA tumors after Gem/nP/αCD40 (Figure 4D). The combination of Gem/nP/αCD40 therapy therefore promotes the development of a robust and orchestrated immune response within the primary tumor site, and allows for CD8⁺ T cell infiltration and destruction of spontaneous KPC tumors, a notoriously difficult site for adaptive immune cells to penetrate.

Gem/nP/αCD40 Therapy Does Not Require Innate Immune Sensors for Efficacy

Because αCD40 can synergize with TLR agonists (Ahonen et al., 2008) and paclitaxel is an LPS mimetic (Ding et al., 1993), we initially hypothesized that Gem/nP/αCD40 efficacy would require TLR4 signaling. We were further attracted to this hypothesis because of previous landmark studies reporting a critical role of TLR4 for chemotherapy-induced anti-tumor immunity (Apetoh et al., 2007). However, when TLR4 KO mice were treated with Gem/nP/αCD40, tumor response rates and growth rates were similar to wild-type mice (Figure 5A). Additionally, robust responses to Gem/nP/αCD40 were also observed in TRIF KO and MyD88 KO mice, indicating that the downstream mediators of TLR4 (as well as all other TLRs) were not required for therapeutic efficacy (Figures 5B and 5C). Caspase 11 (Casp 11) can also function as an intracellular LPS receptor (Shi et al., 2014), but

(C) μMT KO mice. The change in tumor volume on day 24 compared to day 12 is shown on the left. The tumor growth kinetics are shown on the right.

(D–F) Mice were treated as described in Figure 1A, and tumors were harvested on day 15 (24 hr after receiving CD40) and analyzed by flow cytometry with regards to the proportions of indicated subsets among live, CD45⁺ CD3⁻ cells. The CD11c⁺ cells are also CD11b⁻ F4/80⁻.

(G) Batf3 KO mice treated as in Figure 1A. The change in tumor volume on day 24 versus day 12 is shown on the left, and the tumor growth kinetics are shown on the right.

Each bar represents an individual mouse, the symbols indicate groups, and the horizontal lines indicate mean ± SEM (A, C, and G) or each symbol represents an individual mouse, with mean ± SD (B and D–F). Statistical analysis by one-way ANOVA (B and D–F) or two-way ANOVA (A, C, and G) with Tukey's HSD post test is shown. See also Figure S4 and Table S1.

Gem/nP/αCD40 regressed PDA tumors in Casp 11 KO mice the same as wild-type mice (Figure 5D).

Previous reports have shown that ATP released from dying tumor cells stimulates DCs via ATP binding to P2X7R resulting in Casp 1 activation and NLRP3 inflammasome assembly (Ghiringhelli et al., 2009), but P2X7R KO mice bearing PDA tumors responded similarly to Gem/nP/αCD40 therapy as wild-type hosts (Figure 5E). Additionally, we treated tumor-bearing IL-1R KO and Casp 1/11 double KO hosts and found IL-1 signaling was dispensable for treatment efficacy (data not shown). Therefore, we found no role for the inflammasome pathways in mediating the efficacy of Gem/nP/αCD40 therapy.

Previous studies have shown that MyD88/TLR4/P2X7R pathways are not obligatory for immune responses toward tumors in every setting, but rather, the STING pathway can mediate spontaneous or radiation-induced T cell responses against tumors (Deng et al., 2014; Woo et al., 2014). However, STING mutant (STING Mut) mice, which lack STING function, exhibited tumor response rates and growth kinetics similar to wild-type mice after Gem/nP/αCD40 therapy (Figure 5F). Moreover, Type I IFNs (the downstream target of STING activation) were also dispensable, as IFNAR KO hosts responded as well as wild-type hosts to Gem/nP/αCD40 therapy (Figure 5G), despite the role of Type I IFNs in αCD40/TLR agonist peptide vaccines (Ahonen et al., 2004). To exclude the possibility of cancer cell-autonomous signaling of Type I IFNs (Sistigu et al., 2014), we also blocked IFNAR using anti-IFNAR1 mAb and found no reduction in the efficacy of Gem/nP/αCD40 therapy (data not shown). Therefore, we identified no role for STING or downstream Type I IFNs in mediating responses to Gem/nP/αCD40 therapy. We next investigated IL-12, using IL-12p40 or IL-12p35 KO mice, as well as TNF-α, and found that treatment with Gem/nP/αCD40 resulted in tumor responses and growth kinetics similar to wild-type mice receiving therapy (Figure 5H and data not shown).

Thus, Gem/nP/αCD40 treatment is mediated by CD40 and IFN-γ, but independent of 11 other signaling pathways and cytokines, summarized in Table 1. These data illustrate the potency of CD40 stimulation, in combination with Gem/nP, as a non-redundant pathway with the capacity to override the need for classically described innate sensors in mediating activation of anti-tumor immune responses.

DISCUSSION

Although innate immune sensors can play critical roles in spontaneous and therapeutic tumor immunity, here, we demonstrate that CD40 stimulation bypasses the need for TLRs, the inflammasome, Type I IFNs, and STING to generate effective priming of adaptive T cell responses against cancer. Using a mutant KRAS-driven mouse model of PDA, we observed that treatment with an agonistic αCD40 mAb and chemotherapy alters multiple dimensions of the cancer immunity cycle away from immunosuppression and toward T cell-dependent tumor rejection. The ultimate effect is conversion of an otherwise immunologically cold tumor into one with robust T cell infiltration. Mechanistically, αCD40 and chemotherapy activated myeloid cells and drove T cell function, but αCD40 was required to change T cell profiles in the TME and drive expansion of clonal effector T cell responses. Studies using KO mice showed that host CD40 expression is required for efficacy, as is IFN-γ and cross-presenting DCs. Thus, both gain-of-function and loss-of-function studies highlight the non-redundant role of CD40 activation, in combination with Gem/nP, to obviate the need of innate immune sensing for durable anti-cancer T cell immunity.

In contrast to immune checkpoint antibodies that unlock pre-existing T cell immunity against cancer, our data support the notion of αCD40 mAb as a complimentary therapeutic strategy in which immune cells are directly activated using an agonistic mAb (rather than blocking mAb) to achieve T cell priming. Expressed by APCs, CD40 uniquely sits proximal in the T cell activation cascade compared to other activation receptors, such as OX40, GITR, or CD137, the ligands of which are upregulated by CD40 activation (Summers deLuca and Gommerman, 2012). To exploit this pathway pharmaceutically, a number of agonistic CD40 antibodies are being evaluated in cancer clinical trials (Melero et al., 2013; Vonderheide and Glennie, 2013). Our group has shown that one such CD40 mAb (CP-870,893) results in modest rates of objective tumor regression as a single agent in patients with melanoma (Bajor et al., 2014; Vonderheide et al., 2007) in the absence of autoimmune-like events associated with αPD-1 or αCTLA-4 therapy. Nevertheless, studies from tumor-bearing mice predict that αCD40 alone in the absence of a "vaccine" to deliver tumor antigen will be an inefficient therapeutic approach. Indeed, T cell-mediated tumor regressions with αCD40 alone in mice have largely been reported only in immunogenic tumors such as those expressing viral antigens (van Mierlo et al., 2002).

We therefore examined the therapeutic prospect of αCD40 as an immune combination partner in our PDA models with a new standard-of-care Gem/nP chemotherapy. Although the addition of Gem to αCD40 was found to enable T cell immunity against murine mesothelioma (Nowak et al., 2003), in our model of PDA, Gem/αCD40 (without nP) mediates potent T cell immunity against subcutaneous tumors, but not in spontaneous KPC tumors for which the T cell response is restrained by macrophages (Beatty et al., 2011, 2015). Accordingly, Gem/αCD40 therapy resulted in modest tumor regression rates in patients with metastatic PDA, but tumors lacked T cell infiltrates, and all patients eventually progressed (Beatty et al., 2011). Here, using the chemotherapy doublet of Gem/nP, we observed clear evidence of T cell-mediated regression in both subcutaneous and spontaneous KPC tumors, suggesting an immunological benefit of Gem/nP compared to Gem alone. Probing the immunological mechanism underlying Gem/nP/CD40 efficacy, we found that chemotherapy and αCD40 therapy shifted the myeloid compartment toward an M1 bias, and the T cell subsets toward a Th1 bias, in terms of both phenotype and function, with a near complete collapse of the intratumoral T_{Reg} compartment. Importantly, based on TCR deep sequencing of intratumoral T cells, treatment with αCD40 was independently associated with expansion of the top clones within TCR repertoire, as well as the recruitment of new clones to the TME.

Taken together, our findings support a mechanistic model of tumor immunity in which the addition of both Gem and nP converts the effect of αCD40 therapy from macrophage-dependency

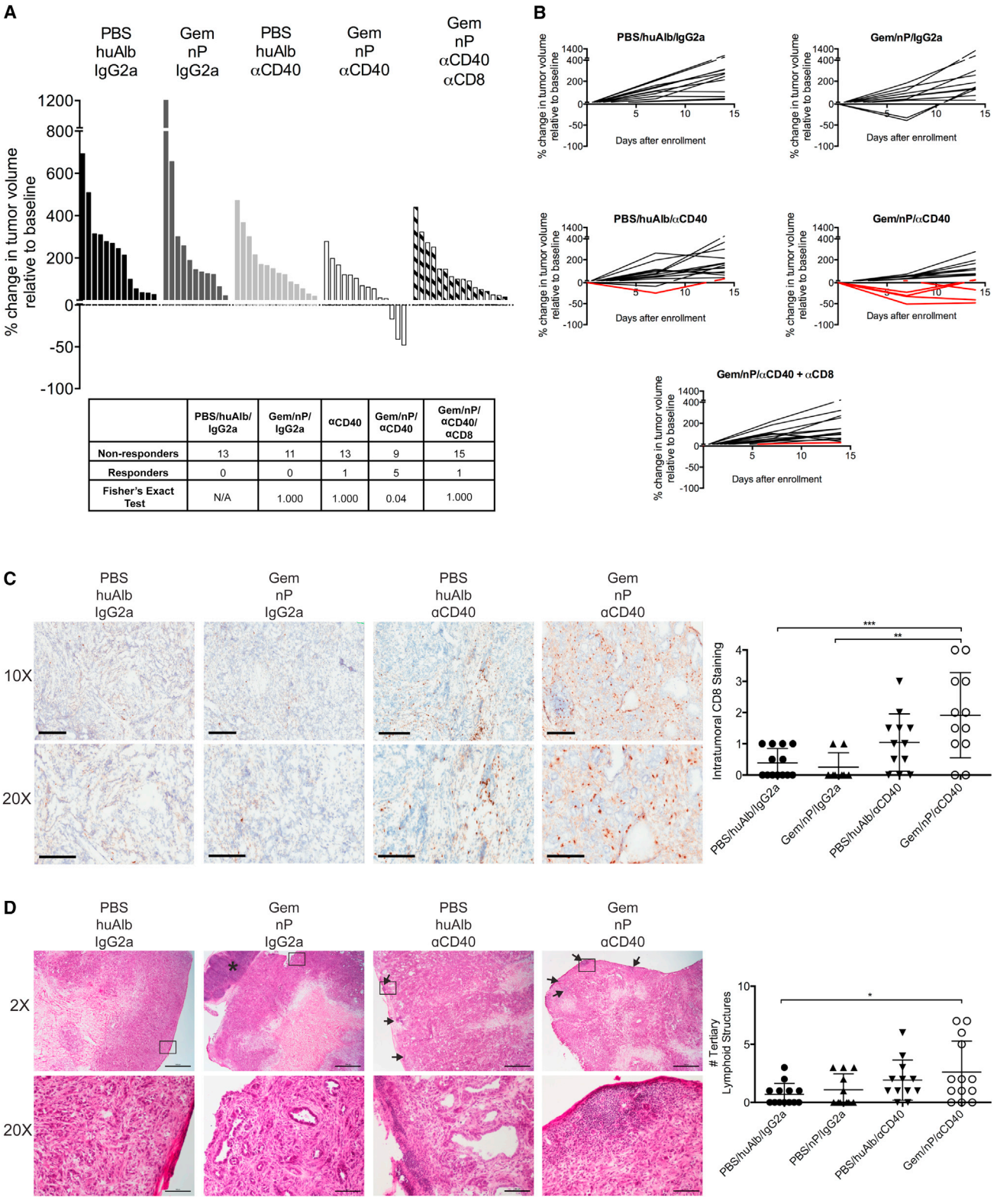

	PBS/huAlb/ IgG2a	Gem/nP/ IgG2a	αCD40	Gem/nP/ αCD40	Gem/nP/ αCD40/ αCD8
Non-responders	13	11	13	9	15
Responders	0	0	1	5	1
Fisher's Exact Test	N/A	1.000	1.000	0.04	1.000

Figure 4. Spontaneous Tumors in KPC Mice Respond to Gem/nP/αCD40 Therapy in T Cell-Dependent Fashion

KPC mice diagnosed with established tumors received Gem/nP on day 0 and day 7 and αCD40 was given on day 2. Some mice (as indicated) also received αCD8 depletion for the duration of enrollment.

(legend continued on next page)

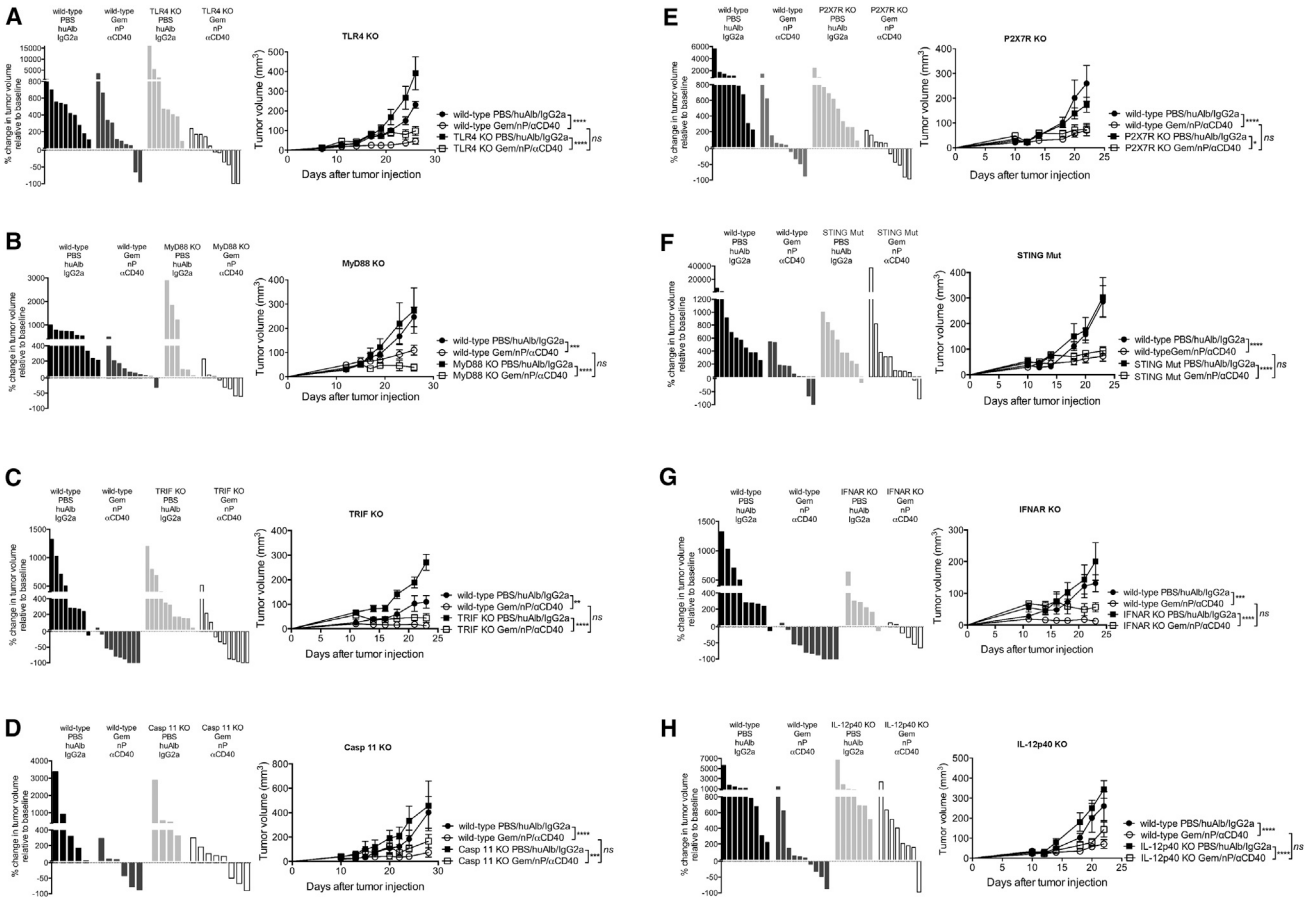

Figure 5. Gem/nP/αCD40 Therapy Bypasses Innate Immune Sensors for Treatment Efficacy

Mice were treated as outlined in Figure 1A, and for each panel: left, change in tumor volume on day 24 compared to day 12 (start of therapy), right, tumor growth kinetics.

(A–H) TLR4 KO (A), MyD88 KO (B), TRIF KO (C), Casp 11 KO (D), P2X7R KO (E), STING Mut (F), IFNAR KO (G), and IL-12p40 KO (H).

Each bar represents a single mouse, each symbol represents a group with error bars indicating mean ± SEM, and the data show representatives of 2–5 independent experiments for each KO strain with 4–10 mice per group. The statistical analysis was by two-way ANOVA with Tukey's HSD post test.

to T cell-dependency. The combination chemotherapy fuels tumor antigen release that cooperates with CD40-mediated DC activation and drives T cell priming. nP, but not Gem, increased tumor cell death shortly after administration so that αCD40 given 2 days later optimally impacts antigen-loaded DCs. Moreover, efficacy of Gem/nP/αCD40 was lost in Batf3 KO mice, which lack DCs most capable of antigen cross-presentation. Thus, insufficient APC activation and antigen presentation—an important immune deficiency in cancer—may be uniquely addressed via αCD40 therapy.

Given the immune benefit from the addition of Gem/nP, it is interesting that classical innate immune sensing—as evaluated in vivo both genetically and pharmacologically—played no role in mediating T cell regression triggered by Gem/nP/αCD40. There were 11 such pathways—including MyD88, P2X7R, and IFNAR—that were tested, but none was found to be required. In certain previous studies, chemotherapy alone induces immunogenic tumor cell death dependent on host MyD88/TLR4 signaling (Apetoh et al., 2007). In other experimental models, response to chemotherapy is independent of the adaptive

(A) The change in tumor volume on day 14 compared to initial tumor volume at diagnosis, responders calculated in table below.

(B) Tumor growth curves for indicated groups, responders indicated in red.

(C) Representative histological samples from (A) at day 14, stained for CD8, shown on left at two magnifications, quantification of global CD8 staining in tumors on right. The scale bar represents 200 μm (top) or 300 μm (bottom).

(D) Representative H&E samples of tumors from (A) at day 14 shown on left, quantification of tertiary lymphoid structures (TLS) in entire tumor section on right. The arrowheads (2×) point to TLS (top), the asterisk indicates a tumor-associated lymph node, and the outline indicates the field below (20×). The scale bar represents 1,000 μm (top) or 100 μm (bottom).

Each bar, line, or symbol represents an individual mouse and the horizontal lines indicate mean ± SD. The statistical analysis by one-way ANOVA with Tukey's HSD post test (C and D) and Fisher's exact test (A) are shown.

Table 1. Gem/nP/αCD40 Is Dependent Only on Host CD40 and IFN-γ, T Cells, and Batf3$^+$ DCs

Target	Response to Gem/nP/αCD40
Signaling Molecules	
CD40	*No*
MyD88	Yes
TLR4	Yes
TRIF	Yes
TLR3	Yes
Caspase 1	Yes
Caspase 11	Yes
STING	Yes
P2X7R	Yes
Cytokines	
IFN-γ	*No*
IFN-α/β	Yes
IL-1	Yes
IL-12	Yes
TNF-α	Yes
Adaptive Immune Cells	
CD4$^+$ T cells	*No*
CD8$^+$ T cells	*No*
B cells	Yes
Innate Immune Cells	
Batf3$^+$ DCs	*No*
NK cells	Yes

Proteins or cells required for therapeutic efficacy are italic.

immune system, particularly in spontaneous mouse tumor models (Ciampricotti et al., 2012), and may require additional modifiers of the TME to trigger T cell responses, e.g., inhibition of CSF-1R (DeNardo et al., 2011; Zhu et al., 2014) or BTK (Massó-Vallés et al., 2015).

Our approach with αCD40 is therapeutically and mechanistically distinct from other strategies to enhance T cell immunity against PDA, offering the potential for further synergistic combinations. For example, FAP$^+$ stromal cells in PDA regulate T cell infiltration to PDA via CXCL12/CXCR4 (Feig et al., 2013), but FAP$^+$ stromal cells in the KPC model are CD40-negative, and FAP$^+$ cell depletion (or CXCR4 inhibition) does not negatively impact T_{Regs} in the way αCD40/chemotherapy does in the same KPC model. Vaccination with recombinant antigen-expressing *Listeria* is another powerful method to generate anti-PDA T cells (Keenan et al., 2014), but appears to rely on STING activation (Jin et al., 2013; Woodward et al., 2010), unlike αCD40. Other treatments that can mediate T cell responses against PDA include GVAX vaccination (Le et al., 2015; Soares et al., 2015), adoptive transfer of antigen-receptor engineered T cells (Stromnes et al., 2015), and CSF-1R inhibition (Zhu et al., 2014). Although antibody blockade of PD-1 (or PD-L1) with or without αCTLA-4 is largely ineffective in treating PDA in mice or patients (Brahmer et al., 2012; Herbst et al., 2014; Twyman-Saint Victor et al., 2015; Winograd et al., 2015; Zhu et al., 2014), PD-1 blockade in mice synergizes with certain T cell therapies in PDA (Feig et al., 2013; Le et al., 2015; Soares et al., 2015; Zhu et al., 2014). Indeed, we have shown that the addition of checkpoint blockade to Gem/nP/αCD40 in tumor-bearing mice enhances survival in both implantable and spontaneous PDA models (Winograd et al., 2015), and here we show the mechanism by which the PDA TME is rendered sensitive to PD-1 and CTLA-4 antibodies used in that study. Taken together, these reports highlight multiple immune vulnerabilities of PDA that can be targeted in a non-redundant fashion in combination with αCD40 in clinical trials (Melero et al., 2013).

Although the T cells generated by Gem/nP/αCD40 mediate tumor regressions and long-term protection, the precise antigens targeted by this response remain unknown. The minimal expression of non-synonymous mutations in our KPC model and the lack of predicted neo-epitopes able to bind MHC class I (n = 0–5 predicted neo-epitopes per tumor; unpublished data) suggests the target peptide-MHC tumor repertoire is mechanistically distinct from that underlying responsiveness to checkpoint blockade. Human PDA also exhibits a scarcity of non-synonymous mutations such that the burden of neo-epitopes may be relatively low compared to carcinogen-induced tumors such as lung carcinoma or melanoma (Alexandrov et al., 2013; Gubin and Schreiber, 2015; Jones et al., 2008; Sausen et al., 2015). Although peptides derived from mutated KRAS can potentially function as tumor-specific antigens (Tran et al., 2015), vaccination against mutated KRAS is unable to slow growth of established PDA tumors (Keenan et al., 2014). It is possible that T cells generated after Gem/nP/αCD40 treatment are specific for self-antigens, but we did not observe autoimmunity or related toxicities in our experiments, suggesting that these potential antigens are not strongly expressed on essential tissues. Given the shared protection between two independent KPC-derived PDA cell lines, our findings justify a reconsideration of self-antigens—as well as "abnormal self-antigens" not derived on the basis of non-synonymous mutations (Cobbold et al., 2013; Ryan et al., 2010)—as potential tumor rejection antigens.

In summary, our findings demonstrate the powerful ability of a single dose of αCD40 to alter T cells in the TME, expand clonal T cell populations, and convert the TME in pancreatic cancer to a site replete with infiltrating T cells. In combination with a novel chemotherapy doublet, αCD40 treatment bypasses innate immune sensors to generate functional APCs and T cells, culminating in durable responses with curative potential, even in a highly immunosuppressive TME. With the goal of rapidly translating these observations to patients, a newly opened clinical trial (http://www.clinicaltrials.gov, #NCT02588443) is evaluating the administration of Gem/nP and αCD40 before and after surgery in patients presenting with resectable PDA.

EXPERIMENTAL PROCEDURES

Mice

KPC mice have been previously described (Hingorani et al., 2005) and were bred and maintained in the specific pathogen-free facility at the University of Pennsylvania. The genetic background of the C57BL/6 KPC mice was assessed at the DartMouse Speed Congenic Core Facility at the Geisel School of Medicine at Dartmouth College, as described in the Supplemental

Information. STING Mut (*Tmem173*^{gt}/J) (Sauer et al., 2011) were kindly provided by Dr. Susan Ross (Perelman School of Medicine, University of Pennsylvania). All wild-type C57BL/6 and other KO mice (Supplemental Information) were purchased from The Jackson Laboratory and/or bred at the University of Pennsylvania. Most experiments with wild-type C57BL/6 mice were performed in female mice, but tumor growth responses were confirmed in male mice. Experiments in KO and KPC mice were performed with mixed gender mice distributed across treatment groups. Animal protocols were reviewed and approved by the Institute of Animal Care and Use Committee at the University of Pennsylvania.

Cell Lines and In Vivo Growth

The mouse pancreatic cancer cell line 4662 was previously described (Lo et al., 2015). PDA cells were used in experiments after 3–5 passages in vitro; C57BL/6 mice received 2.5 × 10^5 PDA cells subcutaneously only if tumor cell viability was >94%. Cell lines were tested by using the Infectious Microbe PCR Amplification Test (IMPACT) and authenticated by the Research Animal Diagnostic Laboratory (RADIL) at the University of Missouri. Tumors were measured thrice weekly by calipers, and the volume was calculated by $(L \times W^2)/2$, where L is the longest diameter and W is the perpendicular diameter. Mice were designated as responders if tumors had regressed 12–14 days after the initiation of treatment.

Drug Preparation

Gem (Hospira) pharmaceutical grade suspension at 38 mg/ml 2′-deoxy-2′,2′-difluorocytidine was diluted to 12 mg/ml in PBS and administered at 120 mg/kg via intraperitoneal (i.p.) injection (Beatty et al., 2011). nP (Abraxane, Celgene) pharmaceutical grade powder was resuspended at 12 mg/ml in PBS and administered at 120 mg/kg i.p. (Frese et al., 2012) or equivalent molar dose of human albumin (huAlb) (Sigma). Gem/nP or huAlb was injected on day 12 after tumor injection in subcutaneous PDA experiments and on days 0 and 7 in KPC mice. Gem and nP were purchased through the Hospital of the University of Pennsylvania Pharmacy.

Monoclonal Antibodies

Mice received 100 μg of either agonist CD40 rat anti-mouse IgG2a mAb (clone FGK45, endotoxin-free), or the isotype control IgG2a mAb (clone 2A3) (Beatty et al., 2011) on day 14 after 4662 injection or day 2 in KPC mice. $CD4^+$ or $CD8^+$ T cells were depleted with 200 μg each of clone GK1.5 or clone 2.43, respectively, injected i.p. on day 10 and repeated every 4 days, or IgG2b isotype control (clone LTF-2). $CD4^+$ and $CD8^+$ T cell depletion was confirmed by staining peripheral blood (data not shown). KPC mice received CD8 depleting antibody starting on day −1 and repeated every 4 days until day 14. All antibodies were purchased from BioXCell.

Tumor Regression Studies in KPC Mice

KPC mice were monitored for spontaneous tumors by ultrasonography every 1–2 weeks using the Vevo 2100 Imaging System with 55 MHz MicroScan Transducer from Visual Sonics. Mice with tumors measuring at least 30 mm^3 were enrolled within 24 hr of baseline imaging using blocked randomization to assign treatment group. Mice were designated as responders if disease was stable (progression <20% compared to baseline) or if tumors regressed 14 days after initiation of treatment.

Preparation of Tissue Samples from Mice

Mice were euthanized either on day 15, 19, 24, or 26 after 4662 injection, and tumors, draining lymph nodes, and spleens were harvested, as indicated. Tumors were minced and incubated for 45 min in 1 mg/ml collagenase V in DMEM at 37°C. Tumors, spleen, and lymph nodes were mechanically dissociated and passed through a 70 μM cell strainer, spleens were incubated in ACK lysis buffer (BioWhittaker), and then tissues were used for flow cytometric analysis as single cell suspensions. Cells were counted using the Beckman Coulter Counter Z2.

Flow Cytometry

Cell surface molecules were analyzed by incubating single cell suspensions of tissues with primary fluorochrome-labeled antibodies at 4°C for 30 min in PBS with 0.5% BSA and 2 mM EDTA. For cytokine production by T cell subsets, samples were incubated for 4–5 hr at 37°C with PMA/ionomycin (Sigma) and Brefeldin A (Sigma). Intracellular staining was done using the Fixation/Permeabilization Kit from eBiosciences. For cytokine production by APCs and myeloid cells, samples were incubated for 4–5 hr with Brefeldin A and Golgistop (BD Biosciences), with 1 μg/ml LPS (Sigma). Antibodies used in flow analysis are described in the Supplemental Information. Flow cytometric analysis was performed on a FACSCanto or LSR II Flow Cytometer (BD Biosciences). Collected data were analyzed using FlowJo software (Treestar).

Immunohistochemistry

Tumors were embedded in optimal cutting temperature compound (OCT) and then sectioned in 5 μm slices, fixed in acetone, and stained using a Bond Max automated staining system (Leica Microsystems), with the Bond Intense R staining kit (Leica Microsystems), using CD8 primary antibody (clone 53-6.7, Abcam). H&E stains were performed according to manufacturer's directions (Sigma). The histopathological scoring is detailed in the Supplemental Information.

TCR Deep Sequencing and Analysis

High-throughput next-generation sequencing of the TCR-β CDR3 region was performed by Adaptive Biotechnologies using the ImmunoSeq platform (Supplemental Information). Analysis of TCR-β repertoire was performed using the tcR R package (Nazarov et al., 2015). Random forest machine learning for classification predictions was performed using the randomForestSRC R package (Ishwaran and Kogalur, 2010) as previously described (Twyman-Saint Victor et al., 2015).

Statistical Analyses

Significance of overall survival was determined using Kaplan-Meier survival curve with log-rank analysis. All other comparisons were performed using one- or two-way ANOVA with Tukey's HSD post test, or Mann-Whitney t test, as indicated. All statistical analyses were performed with Graphpad Prism 6 (GraphPad). SD or SEM shown as indicated by error bars. $p < 0.05$ was considered statistically significant; *$p < 0.05$, ** $p < 0.01$, *** $p < 0.001$, and *** $p < 0.0001$ and ns (or lack of indicated p value) denotes not significant ($p > 0.05$).

SUPPLEMENTAL INFORMATION

Supplemental Information includes Supplemental Experimental Procedures, four figures, and one table and can be found with this article online at http://dx.doi.org/10.1016/j.celrep.2016.05.058.

AUTHOR CONTRIBUTIONS

K.T.B. performed and analyzed the experiments, and K.T.B. and R.H.V. conceived of and designed the experiments, interpreted data, and wrote the manuscript.

ACKNOWLEDGMENTS

Supported by the American Cancer Society 125403-PF-14-135-01-LIB (to K.T.B.), the NIH R01-CA-169123 and Pancreatic Cancer Action Network-American Association for Cancer Research (to R.H.V.), and the Parker Institute for Cancer Immunotherapy (K.T.B. and R.H.V.). We thank Drs. Ben Stanger and Anil Rustgi (Perelman School of Medicine, University of Pennsylvania), Christopher Hunter and Ellen Pure (University of Pennsylvania School of Veterinary Medicine), and Dafna Bar-Sagi (New York University School of Medicine), as well as Andrew Rech, David Bajor, and other members of the R.H.V. laboratory, and Despina Siolas and Jane Cullis from the Bar-Sagi laboratory for helpful discussions.

Received: December 6, 2015
Revised: April 6, 2016
Accepted: May 15, 2016
Published: June 9, 2016

REFERENCES

Ahonen, C.L., Doxsee, C.L., McGurran, S.M., Riter, T.R., Wade, W.F., Barth, R.J., Vasilakos, J.P., Noelle, R.J., and Kedl, R.M. (2004). Combined TLR and CD40 triggering induces potent CD8+ T cell expansion with variable dependence on type I IFN. J. Exp. Med. *199*, 775–784.

Ahonen, C.L., Wasiuk, A., Fuse, S., Turk, M.J., Ernstoff, M.S., Suriawinata, A.A., Gorham, J.D., Kedl, R.M., Usherwood, E.J., and Noelle, R.J. (2008). Enhanced efficacy and reduced toxicity of multifactorial adjuvants compared with unitary adjuvants as cancer vaccines. Blood *111*, 3116–3125.

Alexandrov, L.B., Nik-Zainal, S., Wedge, D.C., Aparicio, S.A., Behjati, S., Biankin, A.V., Bignell, G.R., Bolli, N., Borg, A., Børresen-Dale, A.L., et al.; Australian Pancreatic Cancer Genome Initiative; ICGC Breast Cancer Consortium; ICGC MMML-Seq Consortium; ICGC PedBrain (2013). Signatures of mutational processes in human cancer. Nature *500*, 415–421.

Alvarez, R., Musteanu, M., Garcia-Garcia, E., Lopez-Casas, P.P., Megias, D., Guerra, C., Muñoz, M., Quijano, Y., Cubillo, A., Rodriguez-Pascual, J., et al. (2013). Stromal disrupting effects of nab-paclitaxel in pancreatic cancer. Br. J. Cancer *109*, 926–933.

Apetoh, L., Ghiringhelli, F., Tesniere, A., Obeid, M., Ortiz, C., Criollo, A., Mignot, G., Maiuri, M.C., Ullrich, E., Saulnier, P., et al. (2007). Toll-like receptor 4-dependent contribution of the immune system to anticancer chemotherapy and radiotherapy. Nat. Med. *13*, 1050–1059.

Bajor, D.L., Xu, X., Torigian, D.A., Mick, R., Garcia, L.R., Richman, L.P., Desmarais, C., Nathanson, K.L., Schuchter, L.M., Kalos, M., and Vonderheide, R.H. (2014). Immune activation and a 9-year ongoing complete remission following CD40 antibody therapy and metastasectomy in a patient with metastatic melanoma. Cancer Immunol. Res. *2*, 1051–1058.

Beatty, G.L., Chiorean, E.G., Fishman, M.P., Saboury, B., Teitelbaum, U.R., Sun, W., Huhn, R.D., Song, W., Li, D., Sharp, L.L., et al. (2011). CD40 agonists alter tumor stroma and show efficacy against pancreatic carcinoma in mice and humans. Science *331*, 1612–1616.

Beatty, G.L., Torigian, D.A., Chiorean, E.G., Saboury, B., Brothers, A., Alavi, A., Troxel, A.B., Sun, W., Teitelbaum, U.R., Vonderheide, R.H., and O'Dwyer, P.J. (2013). A phase I study of an agonist CD40 monoclonal antibody (CP-870,893) in combination with gemcitabine in patients with advanced pancreatic ductal adenocarcinoma. Clin. Cancer Res. *19*, 6286–6295.

Beatty, G.L., Winograd, R., Evans, R.A., Long, K.B., Luque, S.L., Lee, J.W., Clendenin, C., Gladney, W.L., Knoblock, D.M., Guirnalda, P.D., and Vonderheide, R.H. (2015). Exclusion of T Cells from pancreatic carcinomas in mice Is regulated by Ly6C(low) F4/80(+) extratumoral macrophages. Gastroenterology *149*, 201–210.

Bennett, S.R., Carbone, F.R., Karamalis, F., Flavell, R.A., Miller, J.F., and Heath, W.R. (1998). Help for cytotoxic-T-cell responses is mediated by CD40 signalling. Nature *393*, 478–480.

Brahmer, J.R., Tykodi, S.S., Chow, L.Q., Hwu, W.J., Topalian, S.L., Hwu, P., Drake, C.G., Camacho, L.H., Kauh, J., Odunsi, K., et al. (2012). Safety and activity of anti-PD-L1 antibody in patients with advanced cancer. N. Engl. J. Med. *366*, 2455–2465.

Ciampricotti, M., Hau, C.S., Doornebal, C.W., Jonkers, J., and de Visser, K.E. (2012). Chemotherapy response of spontaneous mammary tumors is independent of the adaptive immune system. Nat. Med. *18*, 344–346, author reply 346.

Clark, C.E., Hingorani, S.R., Mick, R., Combs, C., Tuveson, D.A., and Vonderheide, R.H. (2007). Dynamics of the immune reaction to pancreatic cancer from inception to invasion. Cancer Res. *67*, 9518–9527.

Cobbold, M., De La Peña, H., Norris, A., Polefrone, J.M., Qian, J., English, A.M., Cummings, K.L., Penny, S., Turner, J.E., Cottine, J., et al. (2013). MHC class I-associated phosphopeptides are the targets of memory-like immunity in leukemia. Sci. Transl. Med. *5*, 203ra125.

Commisso, C., Davidson, S.M., Soydaner-Azeloglu, R.G., Parker, S.J., Kamphorst, J.J., Hackett, S., Grabocka, E., Nofal, M., Drebin, J.A., Thompson, C.B., et al. (2013). Macropinocytosis of protein is an amino acid supply route in Ras-transformed cells. Nature *497*, 633–637.

Corrales, L., and Gajewski, T.F. (2015). Molecular pathways: targeting the stimulator of interferon genes (STING) in the immunotherapy of cancer. Clin. Cancer Res. *21*, 4774–4779.

DeNardo, D.G., Brennan, D.J., Rexhepaj, E., Ruffell, B., Shiao, S.L., Madden, S.F., Gallagher, W.M., Wadhwani, N., Keil, S.D., Junaid, S.A., et al. (2011). Leukocyte complexity predicts breast cancer survival and functionally regulates response to chemotherapy. Cancer Discov. *1*, 54–67.

Deng, L., Liang, H., Xu, M., Yang, X., Burnette, B., Arina, A., Li, X.D., Mauceri, H., Beckett, M., Darga, T., et al. (2014). STING-dependent cytosolic DNA sensing promotes radiation-induced Type I interferon-dependent antitumor immunity in immunogenic tumors. Immunity *41*, 843–852.

Diehl, L., den Boer, A.T., Schoenberger, S.P., van der Voort, E.I., Schumacher, T.N., Melief, C.J., Offringa, R., and Toes, R.E. (1999). CD40 activation in vivo overcomes peptide-induced peripheral cytotoxic T-lymphocyte tolerance and augments anti-tumor vaccine efficacy. Nat. Med. *5*, 774–779.

Dieu-Nosjean, M.C., Goc, J., Giraldo, N.A., Sautès-Fridman, C., and Fridman, W.H. (2014). Tertiary lymphoid structures in cancer and beyond. Trends Immunol. *35*, 571–580.

Ding, A., Sanchez, E., and Nathan, C.F. (1993). Taxol shares the ability of bacterial lipopolysaccharide to induce tyrosine phosphorylation of microtubule-associated protein kinase. J. Immunol. *151*, 5596–5602.

Emens, L.A., and Middleton, G. (2015). The interplay of immunotherapy and chemotherapy: harnessing potential synergies. Cancer Immunol. Res. *3*, 436–443.

Feig, C., Jones, J.O., Kraman, M., Wells, R.J., Deonarine, A., Chan, D.S., Connell, C.M., Roberts, E.W., Zhao, Q., Caballero, O.L., et al. (2013). Targeting CXCL12 from FAP-expressing carcinoma-associated fibroblasts synergizes with anti-PD-L1 immunotherapy in pancreatic cancer. Proc. Natl. Acad. Sci. USA *110*, 20212–20217.

French, R.R., Chan, H.T., Tutt, A.L., and Glennie, M.J. (1999). CD40 antibody evokes a cytotoxic T-cell response that eradicates lymphoma and bypasses T-cell help. Nat. Med. *5*, 548–553.

Frese, K.K., Neesse, A., Cook, N., Bapiro, T.E., Lolkema, M.P., Jodrell, D.I., and Tuveson, D.A. (2012). nab-Paclitaxel potentiates gemcitabine activity by reducing cytidine deaminase levels in a mouse model of pancreatic cancer. Cancer Discov. *2*, 260–269.

Ghiringhelli, F., Apetoh, L., Tesniere, A., Aymeric, L., Ma, Y., Ortiz, C., Vermaelen, K., Panaretakis, T., Mignot, G., Ullrich, E., et al. (2009). Activation of the NLRP3 inflammasome in dendritic cells induces IL-1beta-dependent adaptive immunity against tumors. Nat. Med. *15*, 1170–1178.

Green, D.R., Ferguson, T., Zitvogel, L., and Kroemer, G. (2009). Immunogenic and tolerogenic cell death. Nat. Rev. Immunol. *9*, 353–363.

Gubin, M.M., and Schreiber, R.D. (2015). CANCER. The odds of immunotherapy success. Science *350*, 158–159.

Herbst, R.S., Soria, J.C., Kowanetz, M., Fine, G.D., Hamid, O., Gordon, M.S., Sosman, J.A., McDermott, D.F., Powderly, J.D., Gettinger, S.N., et al. (2014). Predictive correlates of response to the anti-PD-L1 antibody MPDL3280A in cancer patients. Nature *515*, 563–567.

Hingorani, S.R., Wang, L., Multani, A.S., Combs, C., Deramaudt, T.B., Hruban, R.H., Rustgi, A.K., Chang, S., and Tuveson, D.A. (2005). Trp53R172H and KrasG12D cooperate to promote chromosomal instability and widely metastatic pancreatic ductal adenocarcinoma in mice. Cancer Cell *7*, 469–483.

Ishwaran, H., and Kogalur, U.B. (2010). Consistency of random survival forests. Stat. Probab. Lett. *80*, 1056–1064.

Jin, L., Getahun, A., Knowles, H.M., Mogan, J., Akerlund, L.J., Packard, T.A., Perraud, A.L., and Cambier, J.C. (2013). STING/MPYS mediates host defense against Listeria monocytogenes infection by regulating Ly6C(hi) monocyte migration. J. Immunol. *190*, 2835–2843.

Jones, S., Zhang, X., Parsons, D.W., Lin, J.C., Leary, R.J., Angenendt, P., Mankoo, P., Carter, H., Kamiyama, H., Jimeno, A., et al. (2008). Core signaling pathways in human pancreatic cancers revealed by global genomic analyses. Science *321*, 1801–1806.

Kaczanowska, S., Joseph, A.M., and Davila, E. (2013). TLR agonists: our best frenemy in cancer immunotherapy. J. Leukoc. Biol. *93*, 847–863.

Keenan, B.P., Saenger, Y., Kafrouni, M.I., Leubner, A., Lauer, P., Maitra, A., Rucki, A.A., Gunderson, A.J., Coussens, L.M., Brockstedt, D.G., et al. (2014). A Listeria vaccine and depletion of T-regulatory cells activate immunity against early stage pancreatic intraepithelial neoplasms and prolong survival of mice. Gastroenterology *146*, 1784–1794.e6.

Le, D.T., Wang-Gillam, A., Picozzi, V., Greten, T.F., Crocenzi, T., Springett, G., Morse, M., Zeh, H., Cohen, D., Fine, R.L., et al. (2015). Safety and survival with GVAX pancreas prime and Listeria Monocytogenes-expressing mesothelin (CRS-207) boost vaccines for metastatic pancreatic cancer. J. Clin. Oncol. *33*, 1325–1333.

Lo, A., Wang, L.C., Scholler, J., Monslow, J., Avery, D., Newick, K., O'Brien, S., Evans, R.A., Bajor, D.J., Clendenin, C., et al. (2015). Tumor-promoting desmoplasia Is disrupted by depleting FAP-expressing stromal cells. Cancer Res. *75*, 2800–2810.

Long, K.B., Gladney, W.L., Tooker, G.M., Graham, K., Fraietta, J.A., and Beatty, G.L. (2016). IFN-gamma and CCL2 cooperate to redirect tumor-infiltrating monocytes to degrade fibrosis and enhance chemotherapy efficacy in pancreatic carcinoma. Cancer Discov. *6*, 400–413.

Lutz, E.R., Wu, A.A., Bigelow, E., Sharma, R., Mo, G., Soares, K., Solt, S., Dorman, A., Wamwea, A., Yager, A., et al. (2014). Immunotherapy converts nonimmunogenic pancreatic tumors into immunogenic foci of immune regulation. Cancer Immunol. Res. *2*, 616–631.

Massó-Vallés, D., Jauset, T., Serrano, E., Sodir, N.M., Pedersen, K., Affara, N.I., Whitfield, J.R., Beaulieu, M.E., Evan, G.I., Elias, L., et al. (2015). Ibrutinib exerts potent antifibrotic and antitumor activities in mouse models of pancreatic adenocarcinoma. Cancer Res. *75*, 1675–1681.

Melero, I., Grimaldi, A.M., Perez-Gracia, J.L., and Ascierto, P.A. (2013). Clinical development of immunostimulatory monoclonal antibodies and opportunities for combination. Clin. Cancer Res. *19*, 997–1008.

Nazarov, V.I., Pogorelyy, M.V., Komech, E.A., Zvyagin, I.V., Bolotin, D.A., Shugay, M., Chudakov, D.M., Lebedev, Y.B., and Mamedov, I.Z. (2015). tcR: an R package for T cell receptor repertoire advanced data analysis. BMC Bioinformatics *16*, 175.

Neesse, A., Frese, K.K., Chan, D.S., Bapiro, T.E., Howat, W.J., Richards, F.M., Ellenrieder, V., Jodrell, D.I., and Tuveson, D.A. (2014). SPARC independent drug delivery and antitumour effects of nab-paclitaxel in genetically engineered mice. Gut *63*, 974–983.

Nowak, A.K., Robinson, B.W., and Lake, R.A. (2003). Synergy between chemotherapy and immunotherapy in the treatment of established murine solid tumors. Cancer Res. *63*, 4490–4496.

Ridge, J.P., Di Rosa, F., and Matzinger, P. (1998). A conditioned dendritic cell can be a temporal bridge between a CD4+ T-helper and a T-killer cell. Nature *393*, 474–478.

Rook, A.H., Gelfand, J.M., Wysocka, M., Troxel, A.B., Benoit, B., Surber, C., Elenitsas, R., Buchanan, M.A., Leahy, D.S., Watanabe, R., et al. (2015). Topical resiquimod can induce disease regression and enhance T-cell effector functions in cutaneous T-cell lymphoma. Blood *126*, 1452–1461.

Ryan, S.O., Turner, M.S., Gariépy, J., and Finn, O.J. (2010). Tumor antigen epitopes interpreted by the immune system as self or abnormal-self differentially affect cancer vaccine responses. Cancer Res. *70*, 5788–5796.

Sauer, J.D., Sotelo-Troha, K., von Moltke, J., Monroe, K.M., Rae, C.S., Brubaker, S.W., Hyodo, M., Hayakawa, Y., Woodward, J.J., Portnoy, D.A., and Vance, R.E. (2011). The N-ethyl-N-nitrosourea-induced Goldenticket mouse mutant reveals an essential function of Sting in the in vivo interferon response to Listeria monocytogenes and cyclic dinucleotides. Infect. Immun. *79*, 688–694.

Sausen, M., Phallen, J., Adleff, V., Jones, S., Leary, R.J., Barrett, M.T., Anagnostou, V., Parpart-Li, S., Murphy, D., Kay Li, Q., et al. (2015). Clinical implications of genomic alterations in the tumour and circulation of pancreatic cancer patients. Nat. Commun. *6*, 7686.

Schoenberger, S.P., Toes, R.E., van der Voort, E.I., Offringa, R., and Melief, C.J. (1998). T-cell help for cytotoxic T lymphocytes is mediated by CD40-CD40L interactions. Nature *393*, 480–483.

Sharma, P., and Allison, J.P. (2015). The future of immune checkpoint therapy. Science *348*, 56–61.

Shi, J., Zhao, Y., Wang, Y., Gao, W., Ding, J., Li, P., Hu, L., and Shao, F. (2014). Inflammatory caspases are innate immune receptors for intracellular LPS. Nature *514*, 187–192.

Sistigu, A., Yamazaki, T., Vacchelli, E., Chaba, K., Enot, D.P., Adam, J., Vitale, I., Goubar, A., Baracco, E.E., Remédios, C., et al. (2014). Cancer cell-autonomous contribution of type I interferon signaling to the efficacy of chemotherapy. Nat. Med. *20*, 1301–1309.

Soares, K.C., Rucki, A.A., Wu, A.A., Olino, K., Xiao, Q., Chai, Y., Wamwea, A., Bigelow, E., Lutz, E., Liu, L., et al. (2015). PD-1/PD-L1 blockade together with vaccine therapy facilitates effector T-cell infiltration into pancreatic tumors. J. Immunother. *38*, 1–11.

Sotomayor, E.M., Borrello, I., Tubb, E., Rattis, F.M., Bien, H., Lu, Z., Fein, S., Schoenberger, S., and Levitsky, H.I. (1999). Conversion of tumor-specific CD4+ T-cell tolerance to T-cell priming through in vivo ligation of CD40. Nat. Med. *5*, 780–787.

Stromnes, I.M., Schmitt, T.M., Hulbert, A., Brockenbrough, J.S., Nguyen, H.N., Cuevas, C., Dotson, A.M., Tan, X., Hotes, J.L., Greenberg, P.D., and Hingorani, S.R. (2015). T Cells engineered against a native antigen can surmount immunologic and physical barriers to treat pancreatic ductal adenocarcinoma. Cancer Cell *28*, 638–652.

Summers deLuca, L., and Gommerman, J.L. (2012). Fine-tuning of dendritic cell biology by the TNF superfamily. Nat. Rev. Immunol. *12*, 339–351.

Tran, E., Ahmadzadeh, M., Lu, Y.C., Gros, A., Turcotte, S., Robbins, P.F., Gartner, J.J., Zheng, Z., Li, Y.F., Ray, S., et al. (2015). Immunogenicity of somatic mutations in human gastrointestinal cancers. Science *350*, 1387–1390.

Twyman-Saint Victor, C., Rech, A.J., Maity, A., Rengan, R., Pauken, K.E., Stelekati, E., Benci, J.L., Xu, B., Dada, H., Odorizzi, P.M., et al. (2015). Radiation and dual checkpoint blockade activate non-redundant immune mechanisms in cancer. Nature *520*, 373–377.

van Mierlo, G.J., den Boer, A.T., Medema, J.P., van der Voort, E.I., Fransen, M.F., Offringa, R., Melief, C.J., and Toes, R.E. (2002). CD40 stimulation leads to effective therapy of CD40(-) tumors through induction of strong systemic cytotoxic T lymphocyte immunity. Proc. Natl. Acad. Sci. USA *99*, 5561–5566.

Von Hoff, D.D., Ramanathan, R.K., Borad, M.J., Laheru, D.A., Smith, L.S., Wood, T.E., Korn, R.L., Desai, N., Trieu, V., Iglesias, J.L., et al. (2011). Gemcitabine plus nab-paclitaxel is an active regimen in patients with advanced pancreatic cancer: a phase I/II trial. J. Clin. Oncol. *29*, 4548–4554.

Von Hoff, D.D., Ervin, T., Arena, F.P., Chiorean, E.G., Infante, J., Moore, M., Seay, T., Tjulandin, S.A., Ma, W.W., Saleh, M.N., et al. (2013). Increased survival in pancreatic cancer with nab-paclitaxel plus gemcitabine. N. Engl. J. Med. *369*, 1691–1703.

Vonderheide, R.H., and Glennie, M.J. (2013). Agonistic CD40 antibodies and cancer therapy. Clin. Cancer Res. *19*, 1035–1043.

Vonderheide, R.H., Flaherty, K.T., Khalil, M., Stumacher, M.S., Bajor, D.L., Hutnick, N.A., Sullivan, P., Mahany, J.J., Gallagher, M., Kramer, A., et al. (2007). Clinical activity and immune modulation in cancer patients treated with CP-870,893, a novel CD40 agonist monoclonal antibody. J. Clin. Oncol. *25*, 876–883.

Westcott, P.M., Halliwill, K.D., To, M.D., Rashid, M., Rust, A.G., Keane, T.M., Delrosario, R., Jen, K.Y., Gurley, K.E., Kemp, C.J., et al. (2015). The mutational landscapes of genetic and chemical models of Kras-driven lung cancer. Nature *517*, 489–492.

Winograd, R., Byrne, K.T., Evans, R.A., Odorizzi, P.M., Meyer, A.R., Bajor, D.L., Clendenin, C., Stanger, B.Z., Furth, E.E., Wherry, E.J., and Vonderheide, R.H. (2015). Induction of T-cell immunity overcomes complete resistance to PD-1 and CTLA-4 blockade and improves survival in pancreatic carcinoma. Cancer Immunol. Res. *3*, 399–411.

Woo, S.R., Fuertes, M.B., Corrales, L., Spranger, S., Furdyna, M.J., Leung, M.Y., Duggan, R., Wang, Y., Barber, G.N., Fitzgerald, K.A., et al. (2014). STING-dependent cytosolic DNA sensing mediates innate immune recognition of immunogenic tumors. Immunity *41*, 830–842.

Woodward, J.J., Iavarone, A.T., and Portnoy, D.A. (2010). c-di-AMP secreted by intracellular Listeria monocytogenes activates a host type I interferon response. Science *328*, 1703–1705.

Zhu, Y., Knolhoff, B.L., Meyer, M.A., Nywening, T.M., West, B.L., Luo, J., Wang-Gillam, A., Goedegebuure, S.P., Linehan, D.C., and DeNardo, D.G. (2014). CSF1/CSF1R blockade reprograms tumor-infiltrating macrophages and improves response to T-cell checkpoint immunotherapy in pancreatic cancer models. Cancer Res. *74*, 5057–5069.

Zitvogel, L., Apetoh, L., Ghiringhelli, F., and Kroemer, G. (2008). Immunological aspects of cancer chemotherapy. Nat. Rev. Immunol. *8*, 59–73.